

## SUPER-STAR CLUSTERS VERSUS OB ASSOCIATIONS

CARSTEN WEIDNER, IAN A. BONNELL

Scottish Universities Physics Alliance (SUPA), School of Physics and Astronomy, University of St. Andrews, North Haugh, St. Andrews, Fife KY16 9SS, UK

AND

HANS ZINNECKER

Astrophysikalisches Institut Potsdam, An der Sternwarte 16, D-14482 Potsdam, Germany

*Draft version September 18, 2018*

### ABSTRACT

Super Star Clusters ( $M_{\text{ecl}} > 10^5 M_{\odot}$ ) are the largest stellar nurseries in our local Universe, containing hundreds of thousands to millions of young stars within a few light years. Many of these systems are found in external galaxies, especially in pairs of interacting galaxies, and in some dwarf galaxies, but relatively few in disk galaxies like our own Milky Way. We show that a possible explanation for this difference is the presence of shear in normal spiral galaxies which impedes the formation of the very large and dense super star clusters but prefers the formation of loose OB associations possibly with a less massive cluster at the center. In contrast, in interacting galaxies and in dwarf galaxies, regions can collapse without having a large-scale sense of rotation. This lack of rotational support allows the giant clouds of gas and stars to concentrate into a single, dense and gravitationally bound system.

*Subject headings:* ISM: clouds – open clusters and associations: general – galaxies: star clusters: general – galaxies: star formation

### 1. INTRODUCTION

Stars generally form in loose groups or embedded clusters in Giant Molecular Clouds (GMC), each cluster containing a dozen to many million of stars (Tutukov 1978; Zinnecker et al. 1993; Lada & Lada 2003; Kroupa 2005; Allen et al. 2007). These embedded clusters need not to be bound or radially well-defined stellar ensembles and the vast majority of them ( $\sim 90\%$ ) will disperse within about 10 Myr (Tutukov 1978; Lada & Lada 2003). Only a small fraction of these clusters will hatch from the clouds as bound clusters, and after a considerable loss in stellar numbers due to gas expulsion (Goodwin 1997; Goodwin & Bastian 2006; Weidner et al. 2007; Baumgardt & Kroupa 2007). While these embedded clusters vary hugely in their number of stars, their physical sizes are all found to be rather similar with  $R \lesssim 1$  pc (Testi et al. 1998; Gutermuth et al. 2005; Testor et al. 2005; Rathborne et al. 2006; Scheepmaker et al. 2007). As the bulk of the galactic field star populations are probably made from dissolving embedded clusters (Kroupa 1995; Lada & Lada 1995, 2003; Adams & Myers 2001; Allen et al. 2007), studying the formation and evolution of the systems is very important.

When comparing the star cluster populations of the Milky Way (MW) and the Large Magellanic Cloud (LMC), we see that although the stellar populations are similar, the LMC has much more massive clusters than have been found in the MW. The stellar initial mass function (IMF) do not differ beyond the expected statistical variation (Massey 2003; Larson 2002; Wyse et al. 2002; Kroupa 2002). Furthermore, despite the lower metallicity of the LMC and other dwarf galaxies, the mass of the most massive stars does not seem to be any differ-

ent (Weidner & Kroupa 2004; Figer 2005; Oey & Clarke 2005; Koen 2006; Weidner et al. 2010). Surprisingly, it is in the much smaller LMC that we find the largest stellar cluster in the local universe, 30 Doradus. At the center of the roughly 200 pc wide 30 Doradus HII region lies the “star-burst cluster” or super-star cluster (SSC) NGC2070/R136. It contains about half a million stars with an estimated total mass of  $\sim 2 \cdot 10^5 M_{\odot}$ , extrapolated from the  $\approx 50000 M_{\odot}$  in stars from the limited range of 2.1 and 25  $M_{\odot}$  within an area of about 150 pc<sup>2</sup> (Selman et al. 1999; Andersen et al. 2009). On larger scales, Bosch et al. (2009) derive a dynamical mass of  $4.5 \cdot 10^5 M_{\odot}$ . It therefore qualifies as a possible globular cluster precursor. The most-massive star-forming regions known in the MW have only  $\approx 50000 M_{\odot}$  (Westerlund 1, Brandner 2008) to  $\approx 75000 M_{\odot}$  (Arches and Cygnus OB2, Figer et al. 2002; Martins et al. 2008; Wolff et al. 2007; Negueruela et al. 2008; Weidner et al. 2010). Though, as no strict definition of SSC’s exist, the Arches cluster close to the Galactic Center and NGC 3603 ( $\approx 1.3 \cdot 10^4 M_{\odot}$ , Harayama et al. 2008) are sometimes called SSCs. But the most massive clusters in the MW appear to have masses 5 to 10 times smaller than 30 Doradus. It is possible that comparable mass clusters do exist in the MW but are obscured.

Massive or super-star clusters appear more frequent in interacting galaxies and based on our knowledge of the local group, in dwarfs galaxies. For example, in the interacting Antennae galaxies (NGC 4038/4039) Zhang & Fall (1999) found a large number of very massive ( $\gtrsim 10^6 M_{\odot}$ ) SSCs. In Tab. 1 and Fig. 1 are shown the most-massive young ( $< 50$  Myr) star cluster for a sample of local galaxies together with the star-formation rate (SFR) and the type of the galaxy. For the whole sample there seems to be no trend with galaxy type and most-massive star cluster but when restricted only to

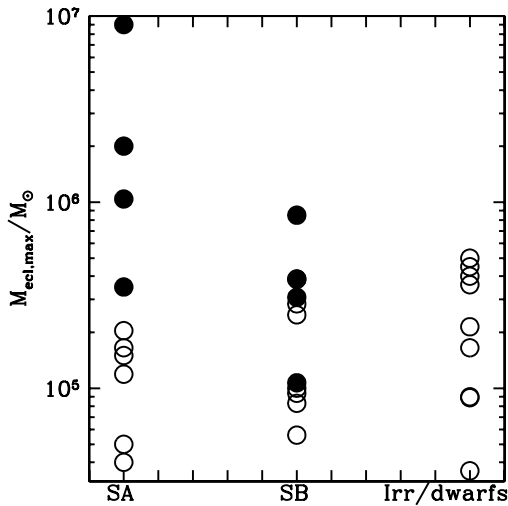


FIG. 1.— Mass of the most-massive young ( $< 50$  Myr) star cluster in nearby spiral, barred spiral and irregular (dwarf) galaxies (see Tab. 1). Filled symbols indicate mergers and galaxies with signs of recent interaction.

non-interacting galaxies (open symbols) there is a clear trend with galaxy type. Irregular and dwarf galaxies, which are systems with less shear, tend to have more massive star clusters than non-interacting spiral galaxies. But due to the small number of objects and large errors in the cluster masses, the statistical significance of the effect is low.

This difference is even more striking when one considers that dwarf galaxies have SFRs 5 to 10 times lower than do spirals, as can be seen by the mean values of the SFR and the maximum cluster mass for different types of galaxies in Tab. 1. A naive speculation would be that such galaxies should only produce lower-mass clusters, when in fact dwarfs appear to produce more massive clusters than (non-interacting) spirals.

One main difference between dwarf galaxies, disk galaxies and interaction regions of galaxies is the amount of shear acting on GMCs in them. While disk galaxies are rotationally supported systems, resulting in relatively large shear forces on GMCs, dwarf galaxies show far less amounts of shear. Interacting galaxies with tidally driven structures are also likely to have low shear in the tidal arms and regions of interaction where SSCs are formed (see also § 2 on more details about shear in disk and dwarf galaxies).

The presence of retrograde rotating GMCs (Blitz 1993) in spiral galaxies is sometimes seen as evidence that the formation and evolution of GMCs is not or only weakly connected to the shear/rotation of spiral arms. In fact Dobbs (2008) has shown that spiral shock models of GMC formation produce both prograde and retrograde rotating GMCs due to the random nature of the coagulation process. Their internal shear is still directly related to that of the galaxy.

In this paper we will examine the influence of different levels of shear on the fragmentation properties of GMCs with masses of  $10^6 M_\odot$ . The model is described in § 2, while § 3 shows the results which are discussed in § 4.

TABLE 1  
MOST-MASSIVE YOUNG ( $< 50$  MYR) STAR CLUSTERS IN GALAXIES OF DIFFERENT TYPES. ‘SA’ INDICATES SPIRAL GALAXIES, ‘SB’ BARRED SPIRALS AND ‘IRR’ IRREGULAR AND DWARFS GALAXIES.

Name	$M_{\text{ecl,max}}$ [ $10^4 M_\odot$ ]	SFR [ $M_\odot \text{ yr}^{-1}$ ]	Type	Ref.
NGC 45	3.6	0.0254	Irr	(1)
NGC 247	8.9	0.0364	Irr	(1)
NGC 1156	9.0	0.186	Irr	(1)
NGC 1569	40.0	0.037	Irr	(1)
NGC 1705	50.0	0.03	Irr	(1)
NGC 5585	21.4	0.0341	Irr	(1)
NGC 7793	16.5	0.141	Irr	(1)
IC 1613	0.3	0.00045	Irr	(2)
LMC	45.0	0.2	Irr	(3)
SMC	36.0	0.15	Irr	(4)
mean	23.0	0.08		
NGC 300	5.0	0.0774	SA	(1)
NGC 628	20.4	0.993	SA	(1)
NGC 3184	16.5	0.395	SA	(1)
NGC 5055	11.9	0.12	SA	(1)
M 31	15.0	0.34	SA	(5)
M 33	4.0	0.21	SA	(6)
mean	12.0	0.35		
NGC 1313	24.8	0.426	SB	(1)
NGC 2403	9.4	0.338	SB	(1)
NGC 2835	8.3	0.0924	SB	(1)
NGC 3521	5.6	2.19	SB	(1)
NGC 7424	28.4	0.173	SB	(1)
MW (Arches)	7.7	1.07	SB	(7)
mean	14.0	0.71		
NGC 2997**	104.0	5.0	SA	(1)
NGC 4038/4039*	200.0	8.3	SA	(8)
NGC 5194*	35.0	4.75	SA	(1)
Arp 220*	900.0	240	SA	(9)
NGC 3621*	38.6	0.881	SB	(1)
NGC 4258*	30.8	0.69	SB	(1)
NGC 5236*	38.6	2.30	SB	(1)
NGC 6744*	10.7	0.434	SB	(1)
NGC 6946**	85.1	2.54	SB	(1)
mean***	68.0	3.1		

\* Interacting or merging galaxy. \*\* Only indirect evidence for a recent interaction in NGC 2997 (Hess et al. 2009) and NGC 6946 (Boomsma et al. 2008). \*\*\* Arp 220 is not included in the mean values for interacting galaxies.

References: 1: Weidner et al. (2004); Larsen (2002, 2009); 2: Wyder et al. (2000); Larsen (2002); 3: Andersen et al. (2009); Harris & Zaritsky (2009); 4: Harris & Zaritsky (2004); Sabbi et al. (2008); 5: Caldwell et al. (2009); Tabatabaei & Berkhuijsen (2010); 6: Thilker et al. (2002); Grossi et al. (2010); 7: Weidner et al. (2010); Robitaille & Whitney (2010); 8: Zhang & Fall (1999); Whitmore et al. (2010); 9: Wilson et al. (2006);

## 2. THE MODEL

The simulations of the gravitational collapse of GMCs under different initial conditions were carried out using a three dimensional (3D) smooth particle hydrodynamics (SPH) code, a Lagrangian hydrodynamics formalism (Monaghan 1992). All clouds started from cold initial conditions in terms of both their thermal and turbulent energies being significantly subvirial and therefore collapse rapidly due to their self-gravity. A barytropic equation-of-state (Larson 2005) is used with  $\gamma = 0.75$  for densities less than  $5.5 \times 10^{-19} \text{ g cm}^{-3}$  and  $\gamma = 1.0$  for densities above. The initial temperature is  $\sim 50$  K and the minimum temperature reached is 7.5 K. The turbulent energies are  $\approx 0.06$  that of the magnitude of the gravitational energies. The details of the initial condi-

tions are summarized in Table 2. In each case the gas is represented by  $10^6$  SPH-particles for the  $10^6 M_\odot$  clouds. To model the star formation, sink particles (Bate et al. 1995) are used which can grow through accretion of infalling gas (SPH particles) and interact gravitationally with the rest of the simulation. The radius of the sink particles is  $r_{\text{sink}} = 0.05$  pc in all four cases. Each sink usually starts with about 50 to  $100 M_\odot$  and can accrete up to  $\sim 5000 M_\odot$  over the length of the simulation. The sinks are therefore not to be seen as a single stars but rather as a small sub-clusters of stars.

The calculations are evolved for about one free-fall time of the GMC. The free-fall time,  $t_{\text{ff}}$ , is the timescale an object needs to collapse from its current radius into a single point under the influence of gravity alone and can be given as (Binney & Tremaine 1987):

$$t_{\text{ff}} = \frac{1}{4} \left( \frac{3\pi}{2G\rho_{\text{GMC}}} \right)^{1/2}, \quad (1)$$

with  $G$  being Newton's gravitational constant and  $\rho_{\text{GMC}}$  the mass density of the GMC. With a radius of  $R_{\text{GMC}} = 50$  pc and a mass  $M_{\text{GMC}} = 10^6 M_\odot$  the free-fall time is  $t_{\text{ff}} = 5.9$  Myr in all cases considered here.

The temporal evolutions of four model-GMCs are studied, each with the same total gas mass ( $M_{\text{GMC}} = 10^6 M_\odot$ ) and radius ( $R_{\text{GMC}} = 50$  pc) but with four different levels of shear. The first model has no shear, while the remaining three have shear levels corresponding to solid body rotation with angular velocities of  $\Omega = 2 \times 10^{-15}$ ,  $5 \times 10^{-15}$  and  $10^{-14}$  rad s $^{-1}$ . The non-rotating model is taken to replicate the shear level expected in either a non-rotating dwarf galaxy or one in which the interaction with another galaxy produces regions of low shear in the tidally-induced spiral arms. For example, in the LMC a low shear value of  $\Omega_{\text{LMC}} \sim 6 \times 10^{-16}$  rad s $^{-1}$  is inferred from the maximum of the rotational velocity curve of its stars (Alves & Nelson 2000).

Models 2-4 represent typical conditions expected in spiral galaxies. The pattern speed of the Milky Way's spiral arms is estimated as  $\Omega_{\text{MW}} \sim 10^{-15}$  rad s $^{-1}$  (Bissantz et al. 2003). In addition, spiral arms compress the gas from different galactocentric radii which will increase the local shear rates by factors of 10 or more. For example, the velocity gradient in the Orion A GMC ( $M_{\text{GMC}} \approx 2 \cdot 10^5 M_\odot$ , Blitz 1991) is about  $0.3 \times 10^{-14}$  rad s $^{-1}$  (Kutner et al. 1977; Bally et al. 1987). For several other GMCs in the Milky Way very similar values have been measured, e.g like Rosette, Mon R1 and W3 have  $0.3$  to  $0.6 \times 10^{-14}$  rad s $^{-1}$  (Thronson et al. 1985; Blitz 1991). Furthermore, values like the MW ones are found for GMCs in the local spiral galaxy M33 (Rosolowsky et al. 2003). All these GMCs have masses from several  $10^4$  to a few  $10^5 M_\odot$ , roughly similar to the GMCs in our numerical study.

The simulations are followed over  $\sim 6$  Myr, where the free-fall time of the cloud is  $t_{\text{ff}} = 5.9$  Myr (see eq. 1). Each model ran for about 2 month on the SUPA Altix computer of the University of St Andrews.

The simulations presented here do not include any feedback from supernovae, radiation or stellar winds. Though, the effects of ionizing radiation (Dale et al. 2005) and stellar winds (Dale & Bonnell 2008) have been studied before. We note that the inclusion of these

sources of feedback in the above models did not have a significant effect on the star formation rate or efficiency.

### 3. RESULTS

The evolution of the four models is shown in Fig. 2. The cloud evolves due to the internal turbulence, forming filamentary structures. These structures contain local regions which are gravitationally unstable and collapse to form sink-particles, localized regions of star formation. As the collapse continues, more sink-particles are formed and these join together in clusters which subsequently merge into one large super-cluster containing over  $10^5 M_\odot$  within 1 pc, and close to  $4 \times 10^5 M_\odot$  within 10 pc.

At 4.3 Myr in Fig. 2 it can be seen that for increasing levels of shear the collapse and fragmentation produces a more distributed population rather than the highly concentrated super-star cluster found in the no-shear run.

All four models are evaluated at a time of about 4.3 Myr (Fig. 2) after the beginning of the calculations. As the first sinks formed slightly after 1 Myr, some of the massive stars will have reached an age of 3 Myr at which point they would explode as a supernova (Meynet & Maeder 2003). We halt the calculations at this point as we do not include feedback in these models.

As can be seen in Fig. 2, there is a strong dependence of the amount and central concentration of stars on the strength of the applied shear. At lower levels of shear, more sinks are formed and they are much more highly concentrated towards the center of the cloud. Figure 3 shows the temporal evolution of the central cluster core in each model. The mass density is calculated in a sphere of  $r_{\text{core}} = 1.0$  pc around the center of mass of all sinks. The models diverge after 3 Myr as rotational support in the shear models halt the central collapse and core formation that occurs in the absence of shear. The no-shear model reaches average central densities in excess of  $6 \times 10^4 M_\odot \text{ pc}^{-3}$ , up to 15 times larger than the runs with shear.

The difference between the models with and without shear are more evident when considering the mass distribution of the resultant clusters and the distribution of local stellar densities (Figs. 4 and 5). In the no shear runs, the cluster contains nearly  $10^5 M_\odot$  inside 0.1 pc whereas the shear runs have a much more distributed population without any significant central condensations. The total stellar masses in all cases, and hence the star formation efficiencies are not drastically dissimilar with star-formation efficiencies (SFE =  $M_{\text{sinks}}/M_{\text{GMC}}$ ) of 44%, 38%, 26% and 18% for model 1 to 4, respectively. It is simply the distribution of the resultant stellar populations which are very different. Also shown in Fig. 4 are five star clusters and OB associations in the MW and the LMC. Especially, the MW objects in the disk (NGC 3603 and Cygnus OB2) seem to follow the high shear calculation quite well while NGC 2070 in the LMC fits the low shear one. The two other MW objects, Arches and Westerlund 1, are found in between the low and high shear run. Interestingly, neither of these objects are in the Galactic disk but Arches is very close to the Galactic center and Westerlund 1 is at the outer edge of the Galactic bar, both tidally very different regions compared to the disk.

A stronger indication is the cumulative mass distribution as a function of local stellar density measured as the

TABLE 2

INITIAL CONDITIONS OF THE FOUR MODELS SHOWN HERE.  $M_{\text{GMC}}$  IS THE INITIAL MASS OF THE GMC,  $R_{\text{GMC}}$  THE INITIAL RADIUS OF THE GMC AND  $\Omega$  THE INITIAL ANGULAR ROTATIONAL VELOCITY.  $\alpha$  AND  $\beta$  DESCRIBE THE FOLLOWING ENERGY EVOLUTION PARAMETERS.  $\alpha = E_{\text{thermal}}/E_{\text{gravitational}}$ ;  $\beta_{\text{turb}} = E_{\text{turbulence}}/E_{\text{gravitational}}$  AND  $\beta_{\text{rot}} = E_{\text{rotational}}/E_{\text{gravitational}}$ . ALSO SHOWN ARE THE MASS IN SINKS,  $M_{4.3\text{Myr}}$ , AND NUMBER OF SINKS,  $N_{4.3\text{Myr}}$ , AFTER 4.3 MYR.

No.	$M_{\text{GMC}}$ $M_{\odot}$	$R_{\text{GMC}}$ pc	$\Omega$ rad s $^{-1}$	$\alpha$	$\beta_{\text{turb}}$	$\beta_{\text{rot}}$	$M_{4.3\text{Myr}}$ $M_{\odot}$	$N_{4.3\text{Myr}}$
1	$1 \times 10^6$	50	0	$4 \times 10^{-3}$	0.059	0.0	$4.4 \times 10^5$	1451
2	$1 \times 10^6$	50	$2 \times 10^{-15}$	$4 \times 10^{-3}$	0.059	0.032	$3.8 \times 10^5$	1326
3	$1 \times 10^6$	50	$5 \times 10^{-15}$	$4 \times 10^{-3}$	0.059	0.158	$2.6 \times 10^5$	1100
4	$1 \times 10^6$	50	$1 \times 10^{-14}$	$4 \times 10^{-3}$	0.059	0.574	$1.8 \times 10^5$	736

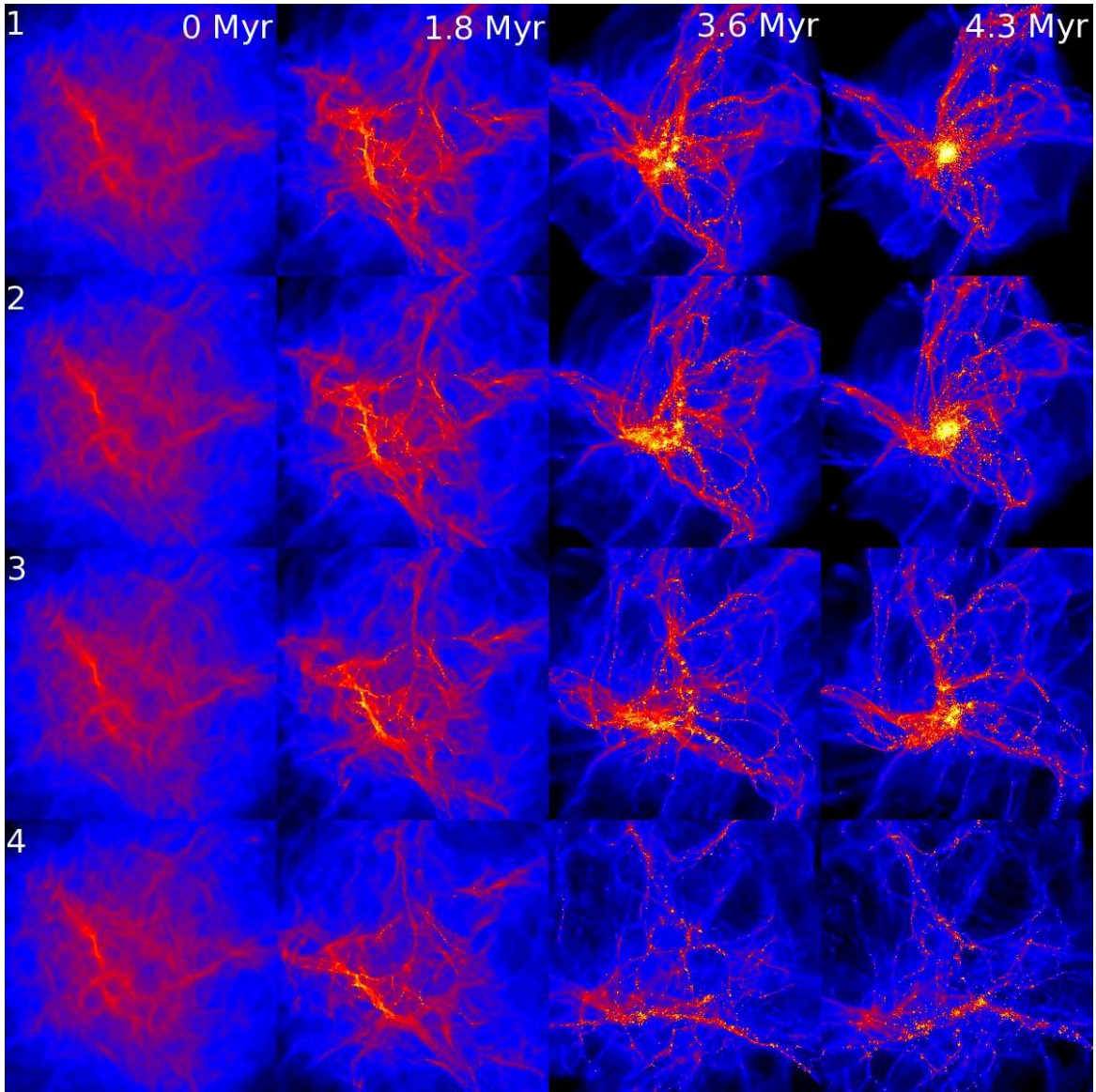


FIG. 2.— Time-evolution series of four models. Each image shows a box of 60 times 60 pc. With increasing shear (model 1 to model 4), the amount and concentration of star-formation decreases.

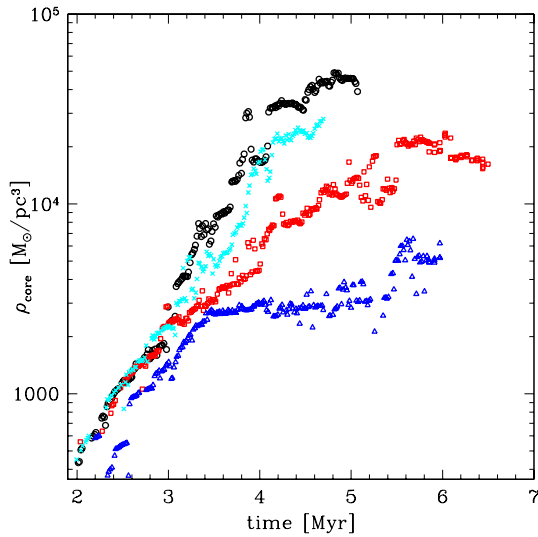


FIG. 3.— Temporal evolution of mass density in a core with  $r_{\text{core}} = 1.0$  pc. The black dots mark model 1, the turquoise crosses model 2, the red boxes model 3 and the blue triangles model 4. After about 3 Myr of very similar evolution of all four models the calculation without shear collapses more quickly and to higher densities. It reaches densities which are about 3 to 15 times larger than those in the runs with shear.

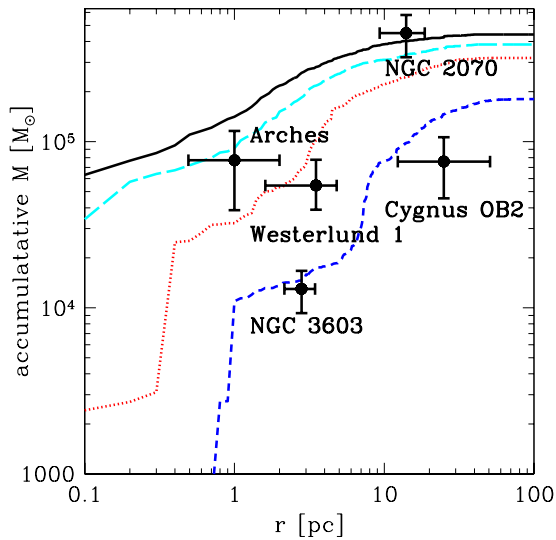


FIG. 4.— The radial dependence of the accumulated mass for all four simulations after 4.3 Myr. The solid black line is for model 1 (no shear), the long-dashed turquoise line for model 2 (some shear), the dotted red line for model 3 (intermediate shear) and the dashed blue line for model 4 (high shear). Also shown are several star clusters in the MW and NGC 2070 in the LMC. The masses are from Weidner et al. (2010).

density of the ten nearest-neighbors of each sink shown in Figure 5. From this we see that approximately  $10^5 M_{\odot}$  is in stars which have local densities from  $10^6$  to  $10^8 M_{\odot} \text{pc}^{-3}$  in the no shear run whereas in the highest shear run, less than  $10^4 M_{\odot}$  is in stars which have local densities

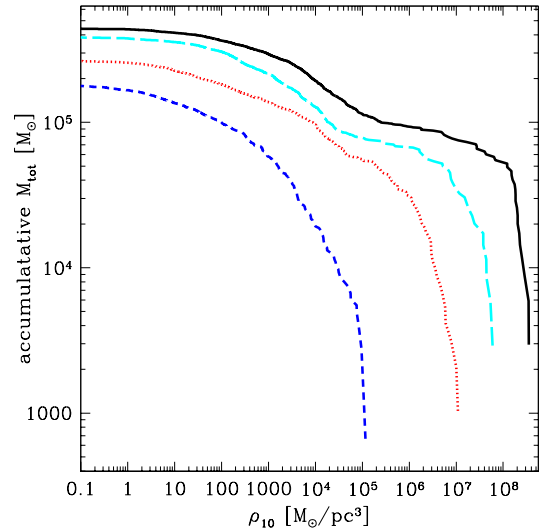


FIG. 5.— The dependence of the accumulated mass on the density derived from the ten nearest neighbors of each sink for all four simulations after 4.3 Myr. The solid black line is for model 1 (no shear), the long-dashed turquoise line for model 2 (some shear), the dotted red line for model 3 (intermediate shear) and the dashed blue line for model 4 (high shear). Clearly, the SPH-calculation without shear accumulates the most mass and this mass is very concentrated compared to the other three cases.

approaching  $10^5 M_{\odot} \text{pc}^{-3}$ . Clearly, the SPH-calculation without shear accumulates the most mass and this mass is very concentrated compared to the other three cases.

For the analysis of the simulations, each time step the center of mass is derived by searching for the highest mass density not of the individual sink but of the ten nearest neighbors. As can be seen in the right panel of Fig. 5 the local mass density reaches rather high values ( $> 10^8 M_{\odot} \text{pc}^{-3}$ ), which is to be expected when, e.g., twenty sinks of masses  $\sim 400 M_{\odot}$  are inside 0.025 pc. Even in the relatively small ( $\sim 2000 M_{\odot}$ , Hillenbrand & Hartmann 1998) Orion Nebula Cluster (ONC), roughly comparable stellar densities are found. The projected radius of the 4 Trapezium stars in the ONC is about 10 arc-seconds, which translates to 0.02 to 0.025 pc for assumed distances to the ONC of 400 to 500 pc (Muench et al. 2008). The combined mass of these four systems (all four stars are binaries or higher-order multiples) is  $\sim 100 M_{\odot}$  (Preibisch et al. 1999; Kraus et al. 2009). Therefore, the stellar density is of the order of  $10^6 M_{\odot} \text{pc}^{-3}$ . A second point is that below 0.05 pc the gravity in the SPH calculation is smoothed and hence 2-body interactions do not occur and systems are stable where otherwise they need not to be. The sinks can cluster well within 0.05 pc and not feel each other directly and hence be stable. Therefore, while the local mass density might be overestimated at times in the calculations, the main point still holds that large amounts of mass are concentrated at high stellar densities in the no-shear run.

#### 4. DISCUSSION

Our simulations show the formation of super-star clusters can depend strongly on the shear content in the pre-

collapse giant molecular cloud. Clouds which are only slowly rotating or not rotating at all, as to be expected in dwarf galaxies like the LMC and in interaction regions of colliding galaxies, can collapse monolithically into a single massive star cluster. This is in agreement with the results by Escala & Larson (2008) who predict the precursors of globular clusters to form only in galaxies not stabilized by rotation.

In contrast, in our calculations clouds in disk galaxies are more prone to fragmentation and form a system of smaller clusters or structures that could evolve to become OB associations or relatively large clusters susceptible to the tidal field of the galaxy with an extended halo of stars. Interestingly, in HST observations of massive extragalactic clusters Maíz-Apellániz (2001) finds a similar result. Four galaxies (NGC 2403, NGC 1569, NGC 1705, LMC) of that study are in common with Tab. 1. For these, the brightest, most compact clusters are all in dwarfs whereas the brightest objects in the normal spiral NGC 2403 are more extended, classified as so-called scaled OB associations.

Although the results of the numerical calculations do not exclude the possibility of SSCs formation in disk galaxies, but they show that the presence of shear in disk galaxies acts to impede the formation of very massive clusters. It is therefore unlikely that the massive clusters which were the progenitors of the present day globular clusters have formed in the disk of galaxies. They might have formed either during an initial monolithic collapse

which formed the bulge of the galaxy, in a major merging event, or they have been accreted from dwarf galaxies (Zinnecker et al. 1988).

The differences between the runs with and without shear cannot be solely attributed to a delay in the evolution. The rotational support in the high shear runs is not negligible and would remain important over large timescales. Furthermore, supernova explosions would be expected to occur in the clusters, halting any further star-formation and potentially unbinding the cluster. But further studies including the different feedback mechanisms are necessary to verify this assumption.

One interesting feature of the high shear run is shown in Fig. 6. While no feedback (like supernovae or stellar winds) is included in the calculations, the high-shear run has a very distinct shell or bubble like feature in the upper part of the figure. Additionally, several sinks are found concentrated along the rim of this feature. Such a structure is easily mistaken as a supernova bubble. The overall appearance of the GMC is now like a system of small star clusters with some amount of distributed star formation around, as seen in several OB associations in the Milky Way.

This work was financially supported by the CONSTELLATION European Commission Marie Curie Research Training Network (MRTN-CT-2006-035890).

#### REFERENCES

- Adams, F. C., & Myers, P. C. 2001, *ApJ*, 553, 744  
 Allen, L., et al. 2007, in *Protostars and Planets V*, ed. B. Reipurth, D. Jewitt, & K. Keil, 361–376  
 Alves, D. R., & Nelson, C. A. 2000, *ApJ*, 542, 789  
 Andersen, M., Zinnecker, H., Moneti, A., McCaughrean, M. J., Brandl, B., Brandner, W., Meylan, G., & Hunter, D. 2009, *ApJ*, 707, 1347  
 Bally, J., Langer, W. D., Stark, A. A., & Wilson, R. W. 1987, *ApJ*, 312, L45  
 Bate, M. R., Bonnell, I. A., & Price, N. M. 1995, *MNRAS*, 277, 362  
 Baumgardt, H., & Kroupa, P. 2007, *MNRAS*, 380, 1589  
 Binney, J., & Tremaine, S. 1987, *Galactic dynamics* (Princeton, NJ, Princeton University Press, 1987, 747 p.)  
 Bissantz, N., Englmaier, P., & Gerhard, O. 2003, *MNRAS*, 340, 949  
 Blitz, L. 1991, in *NATO ASIC Proc. 342: The Physics of Star Formation and Early Stellar Evolution*, ed. C. J. Lada & N. D. Kylafis, 3–+  
 Blitz, L. 1993, in *Protostars and Planets III*, ed. E. H. Levy & J. I. Lunine, 125–161  
 Boomsma, R., Oosterloo, T. A., Fraternali, F., van der Hulst, J. M., & Sancisi, R. 2008, *A&A*, 490, 555  
 Bosch, G., Terlevich, E., & Terlevich, R. 2009, *AJ*, 137, 3437  
 Brandner, W. 2008, in *Astronomical Society of the Pacific Conference Series*, Vol. 387, *Massive Star Formation: Observations Confront Theory*, ed. H. Beuther, H. Linz, & T. Henning, 369–+  
 Caldwell, N., Harding, P., Morrison, H., Rose, J. A., Schiavon, R., & Kriessler, J. 2009, *AJ*, 137, 94  
 Dale, J. E., & Bonnell, I. A. 2008, *MNRAS*, 391, 2  
 Dale, J. E., Bonnell, I. A., Clarke, C. J., & Bate, M. R. 2005, *MNRAS*, 358, 291  
 Dobbs, C. L. 2008, *MNRAS*, 391, 844  
 Escala, A., & Larson, R. B. 2008, *ApJ*, 685, L31  
 Figer, D. F. 2005, *Nature*, 434, 192  
 Figer, D. F., et al. 2002, *ApJ*, 581, 258  
 Goodwin, S. P. 1997, *MNRAS*, 284, 785  
 Goodwin, S. P., & Bastian, N. 2006, *MNRAS*, 373, 752  
 Grossi, M., Corbelli, E., Giovanardi, C., & Magrini, L. 2010, *A&A*, in press (arXiv:1006.1281)  
 Gutermuth, R. A., Megeath, S. T., Pipher, J. L., Williams, J. P., Allen, L. E., Myers, P. C., & Raines, S. N. 2005, *ApJ*, 632, 397  
 Harayama, Y., Eisenhauer, F., & Martins, F. 2008, *ApJ*, 675, 1319  
 Harris, J., & Zaritsky, D. 2004, *AJ*, 127, 1531  
 —. 2009, *AJ*, 138, 1243  
 Hess, K. M., Pisano, D. J., Wilcots, E. M., & Chengalur, J. N. 2009, *ApJ*, 699, 76  
 Hillenbrand, L. A., & Hartmann, L. W. 1998, *ApJ*, 492, 540  
 Koen, C. 2006, *MNRAS*, 365, 590

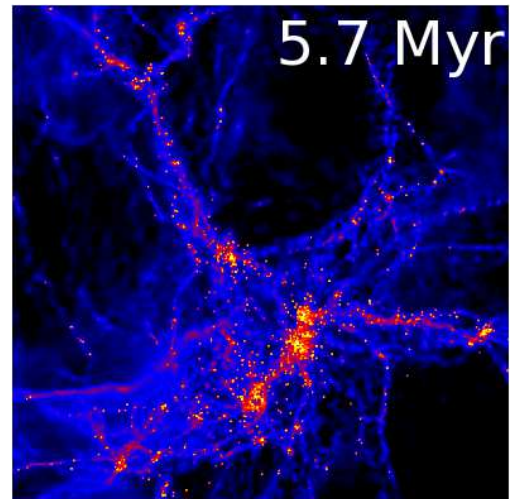


FIG. 6.— The high shear GMC run (model 4) after  $0.968 t_{\text{ff}}$  (5.7 Myr). The image shows a box of 100 times 100 pc. Note the large shell-like gas structure in the upper half of the image which has associated star-formation along its rim. Even without any feedback in the simulation this feature looks like a supernova blown wind-bubble which apparently drives star-formation.

- Kraus, S., et al. 2009, *A&A*, 497, 195
- Kroupa, P. 1995, *MNRAS*, 277, 1491
- . 2002, *Science*, 295, 82
- Kroupa, P. 2005, in *ESA SP-576: The Three-Dimensional Universe with Gaia*, ed. C. Turon, K. S. O’Flaherty, & M. A. C. Perryman (ESA Publications Division, Noordwijk, The Netherlands), 629+– (astro-ph/0412069)
- Kutner, M. L., Tucker, K. D., Chin, G., & Thaddeus, P. 1977, *ApJ*, 215, 521
- Lada, C. J., & Lada, E. A. 2003, *ARA&A*, 41, 57
- Lada, E. A., & Lada, C. J. 1995, *AJ*, 109, 1682
- Larsen, S. S. 2002, *AJ*, 124, 1393
- . 2009, *A&A*, 494, 539
- Larson, R. B. 2002, in *Astronomical Society of the Pacific Conference Series*, Vol. 285, *Modes of Star Formation and the Origin of Field Populations*, ed. E. K. Grebel & W. Brandner, 442+–
- Larson, R. B. 2005, *MNRAS*, 359, 211
- Maíz-Apellániz, J. 2001, *ApJ*, 563, 151
- Martins, F., Hillier, D. J., Paumard, T., Eisenhauer, F., Ott, T., & Genzel, R. 2008, *A&A*, 478, 219
- Massey, P. 2003, *ARA&A*, 41, 15
- Meynet, G., & Maeder, A. 2003, *A&A*, 404, 975
- Monaghan, J. J. 1992, *ARA&A*, 30, 543
- Muench, A., Getman, K., Hillenbrand, L., & Preibisch, T. 2008, *Star Formation in the Orion Nebula I: Stellar Content*, ed. Reipurth, B. (ASP Monograph Publications, San Francisco, USA), 483+–
- Negueruela, I., Marco, A., Herrero, A., & Clark, J. S. 2008, *A&A*, 487, 575
- Oey, M. S., & Clarke, C. J. 2005, *ApJ*, 620, L43
- Preibisch, T., Balega, Y., Hofmann, K.-H., Weigelt, G., & Zinnecker, H. 1999, *New Astronomy*, 4, 531
- Rathborne, J. M., Jackson, J. M., & Simon, R. 2006, *ApJ*, 641, 389
- Robitaille, T. P., & Whitney, B. A. 2010, *ApJ*, 710, L11
- Rosolowsky, E., Engargiola, G., Plambeck, R., & Blitz, L. 2003, *ApJ*, 599, 258
- Sabbi, E., et al. 2008, *AJ*, 135, 173
- Scheepmaker, R. A., Haas, M. R., Gieles, M., Bastian, N., Larsen, S. S., & Lamers, H. J. G. L. M. 2007, *A&A*, 469, 925
- Selman, F., Melnick, J., Bosch, G., & Terlevich, R. 1999, *A&A*, 347, 532
- Tabatabaei, F. S., & Berkhuijsen, E. M. 2010, *A&A*, 517, A77+–
- Testi, L., Palla, F., & Natta, A. 1998, *A&AS*, 133, 81
- Testor, G., Lemaire, J. L., Kristensen, L. E., & Field, D. 2005, in *SF2A-2005: Semaine de l’Astrophysique Française*, ed. F. Casoli, T. Contini, J. M. Hameury, & L. Pagani, 401+–
- Thilker, D. A., Walterbos, R. A. M., Braun, R., & Hoopes, C. G. 2002, *AJ*, 124, 3118
- Thronson, Jr., H. A., Lada, C. J., & Hewagama, T. 1985, *ApJ*, 297, 662
- Tutukov, A. V. 1978, *A&A*, 70, 57
- Weidner, C., & Kroupa, P. 2004, *MNRAS*, 348, 187
- Weidner, C., Kroupa, P., & Bonnell, I. A. 2010, *MNRAS*, 401, 275
- Weidner, C., Kroupa, P., & Larsen, S. S. 2004, *MNRAS*, 350, 1503
- Weidner, C., Kroupa, P., Nürnberger, D. E. A., & Sterzik, M. F. 2007, *MNRAS*, 376, 1879
- Whitmore, B. C., et al. 2010, *AJ*, 140, 75
- Wilson, C. D., Harris, W. E., Longden, R., & Scoville, N. Z. 2006, *ApJ*, 641, 763
- Wolff, S. C., Strom, S. E., Dror, D., & Venn, K. 2007, *AJ*, 133, 1092
- Wyder, T. K., Hodge, P. W., & Cole, A. 2000, *PASP*, 112, 594
- Wyse, R. F. G., Gilmore, G., Houdashelt, M. L., Feltzing, S., Hebb, L., Gallagher, J. S., & Smecker-Hane, T. A. 2002, *New Astronomy*, 7, 395
- Zhang, Q., & Fall, S. M. 1999, *ApJ*, 527, L81
- Zinnecker, H., Keable, C. J., Dunlop, J. S., Cannon, R. D., & Griffiths, W. K. 1988, in *IAU Symposium*, Vol. 126, *The Harlow-Shapley Symposium on Globular Cluster Systems in Galaxies*, ed. J. E. Grindlay & A. G. D. Philip, 603+–
- Zinnecker, H., McCaughrean, M. J., & Wilking, B. A. 1993, in *Protostars and Planets III*, ed. E. H. Levy & J. I. Lunine, 429–495